Arctic Ocean Primary Productivity: The Response of Marine Algae to Climate Warming and Sea Ice Decline

K. E. Frey[1], J. C. Comiso[2], L. W. Cooper[3], J. M. Grebmeier[3], L. V. Stock[2]

[1]Graduate School of Geography, Clark University, Worcester, MA, USA
[2]Cryospheric Sciences Laboratory, NASA Goddard Space Flight Center, Greenbelt, MD, USA
[3]Chesapeake Biological Laboratory, University of Maryland Center for Environmental Science, Solomons, MD, USA

Highlights

- Satellite estimates of ocean primary productivity (i.e., the rate at which marine algae transform dissolved inorganic carbon into organic material) were higher in 2018 (relative to the 2003-17 mean) for three of the nine investigated regions (the Eurasian Arctic, Bering Sea, and Baffin Bay).
- All regions continue to exhibit positive trends over the 2003-18 period, with the strongest trends for the Eurasian Arctic, Barents Sea, Greenland Sea, and North Atlantic.
- The regional distribution of relatively high (low) chlorophyll-*a* concentrations can often be associated with a relatively early (late) breakup of sea ice cover.

Autotrophic single-celled algae living in the sea ice (ice algae) and water column (phytoplankton) are the main primary producers in the Arctic Ocean. Through photosynthesis, they transform dissolved inorganic carbon into organic material. Consequently, primary production provides a key ecosystem service by providing energy to the entire food web in the oceans. The global oceans play a significant role in global carbon budgets via photosynthesis, contributing approximately half of Earth's net annual photosynthesis with ~10-15% of this production occurring on the continental shelves alone (Müller-Karger et al., 2005). Primary productivity is strongly dependent upon light availability and the presence of nutrients, and thus is highly seasonal in the Arctic. In particular, the melting and retreat of sea ice during spring are strong drivers of primary production in the Arctic Ocean and its adjacent shelf seas owing to enhanced light availability and stratification (Barber et al., 2015; Leu et al., 2015; Ardyna et al., 2017). Recent declines in Arctic sea ice extent (see the essay on *Sea Ice*) have contributed substantially to shifts in primary productivity throughout the Arctic Ocean. However, the response of primary production to sea ice loss has been both seasonally and spatially variable (e.g., Tremblay et al., 2015; Hill et al., 2018).

Here we present satellite-based estimates of algal chlorophyll-*a* (occurring in all species of phytoplankton), based on the color of the ocean, and subsequently provide calculated primary production estimates. These results are shown for ocean areas with less than 15% sea ice concentration and, therefore, do not include production by sea ice algae, open water from within the sea ice pack, or under-ice phytoplankton blooms.

Chlorophyll-*a*

Measurements of the algal pigment chlorophyll (e.g., chlorophyll-*a*) serve as a proxy for the amount of algal biomass present as well as overall plant health. The complete, updated MODIS-Aqua satellite chlorophyll-*a* record for the northern polar region for the years 2003-18 can serve as a time-series against which individual years can be compared. For example, a base period of 2003-17 was chosen to calculate the 2018 anomalies to maximize the length of the short satellite-based time series.

The 2018 data show a distribution of both positive and negative anomalies in chlorophyll-*a* concentrations in a number of locations across the Arctic Ocean region, where patterns are spatially and temporally heterogeneous (**Fig. 1**). These patterns are often associated with the timing of sea ice break-up: positive anomalies tend to occur in regions where the break up is relatively early, while negative anomalies tend to occur in regions where the break up is delayed. The most notable positive anomalies in 2018 occurred during May and June, with relatively high concentrations of chlorophyll-*a* occurring in the northern Barents Sea surrounding Svalbard and along the ice edge in the Greenland Sea (**Fig. 1a, b**). These anomalies are associated with clear declines in sea ice cover in these regions as well (**Fig. 2a, b**). Additional widespread positive anomalies occurred in the Bering Sea in June, which will be discussed in greater detail below. Some of the

strongest negative anomalies in chlorophyll-*a* concentrations occurred southeast of Greenland in the Denmark Strait in May and July (**Fig. 1a, c**) and in the Kara Sea in July (**Fig. 1c**). The relatively low chlorophyll-*a* concentrations in the Kara Sea in July are associated with increases in sea ice cover in that region throughout the season (**Fig. 2a-c**).

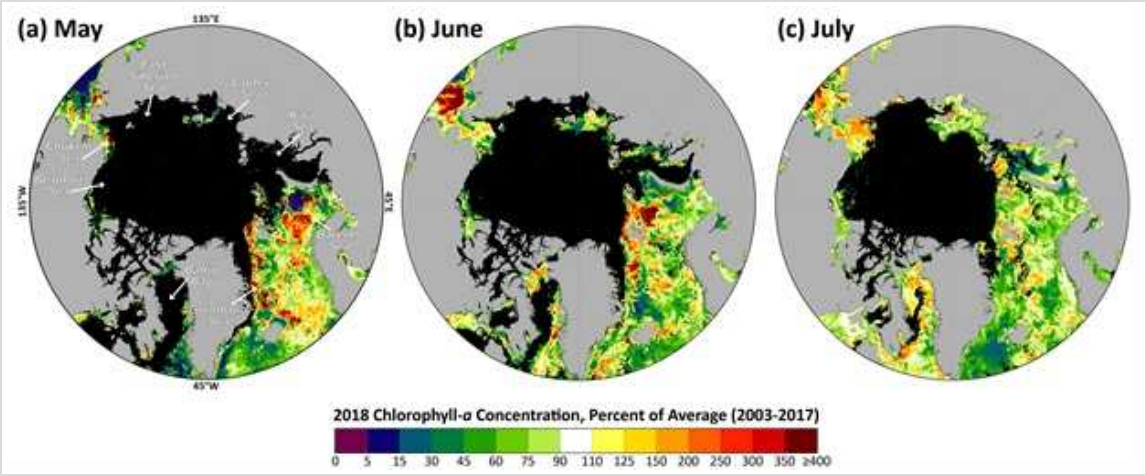

Fig. 1. Mean monthly chlorophyll-*a* concentrations during 2018, shown as a percent of the 2003-17 average for (a) May, (b) June, and (c) July. Satellite-based chlorophyll-*a* data across the pan-Arctic region were derived using the MODIS-Aqua Reprocessing 2014.0, OC3 algorithm: http://oceancolor.gsfc.nasa.gov/.

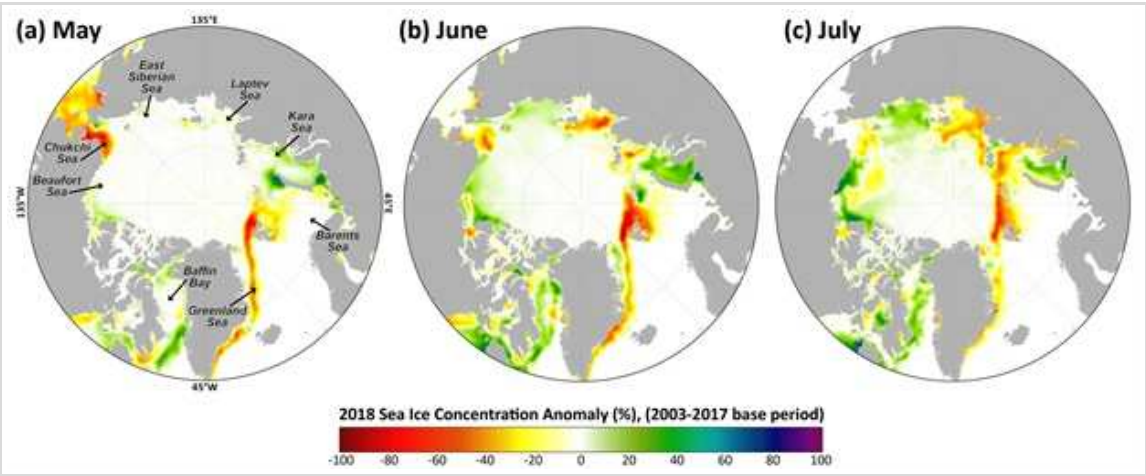

Fig. 2. Sea ice concentration anomalies (%) in 2018 (compared to a 2003-17 mean base period) for (a) May, (b) June, and (c) July. Satellite-based sea ice concentrations were derived from the Special Sensor Microwave/Imager (SSM/I) and Special Sensor Microwave Imager/Sounder (SSMIS) passive microwave instruments, calculated using the Goddard Bootstrap (SB2) algorithm (Comiso et al., 2017a, b).

As noted above, some of the largest positive anomalies in chlorophyll-*a* concentrations observed in 2018 occurred over the shelf region of the Bering Sea during June (**Fig. 3a**). Focusing in on the Pacific Arctic region, these positive anomalies are distributed across the Bering Sea shelf and range from ~400 to 500% of the 2003-17 average. This is in contrast to the negative anomalies in the Bering Sea south of the shelf break that average only ~20% of the 2003-17 average (**Fig. 3a**). In particular, focusing on the Distributed Biological Observatory Site 1 (DBO1; Moore and Grebmeier, 2018) in the St. Lawrence Island Polynya (SLIP) region, it is also apparent that the typical large blooms that occur in April and May did not occur in 2018; instead, we observe a redistribution of chlorophyll biomass in March (~275% increase over the 2003-17 average) and June (~500% increase over the 2003-17 average) (**Fig. 3b**).

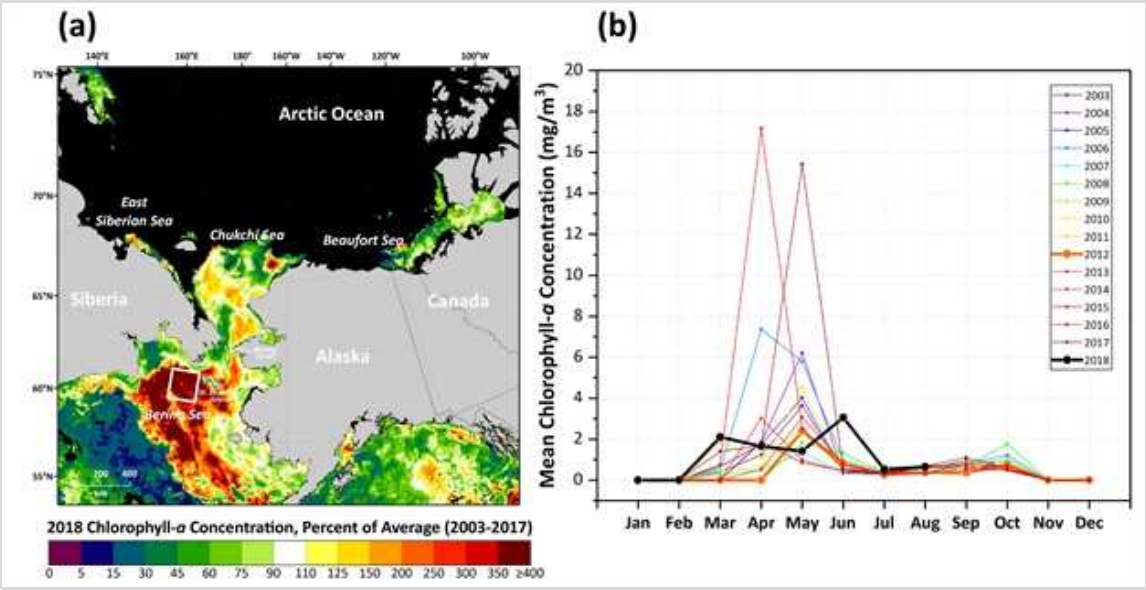

Fig. 3. (a) Mean chlorophyll-*a* concentrations in the Pacific Arctic region during June 2018, shown as a percent of the 2003-17 average. The white box denotes the Distributed Biological Observatory (DBO) Site 1, encompassing the St. Lawrence Island Polynya (SLIP) region. (b) Mean chlorophyll-*a* concentrations for the DBO1/SLIP region from 2003-18, highlighting 2012 (one of the highest years of sea ice cover on record) and 2018 (the lowest year of sea ice cover on record).

This redistribution of the seasonal variability of chlorophyll biomass is of particular interest because this region experienced unprecedented declines in sea ice over the winter of 2018 (**Fig. 4**). For example, DBO1 on average (1981-2010) experiences ~149 days of sea ice cover per year, but in 2018 only had ~20 days of sea ice cover as a result of both later sea ice freeze-up and earlier sea ice break-up (**Fig. 4a, b**). Having knowledge of how regions experience changes in chlorophyll-*a* concentrations with such dramatic losses of sea ice cover will give insight into what to expect with future sea ice declines. In this particular instance, it is important to note that we do not observe simple overall increases in chlorophyll biomass with the unprecedented declines in Bering Sea ice in 2018, but rather a dampening of the large blooms typical of April-May and a redistribution of production in March and June. While many of these observed patterns are directly linked to sea ice variability (and therefore light availability), it is important to note that there are other dominant factors at play that add to the complexity of observed chlorophyll-*a* concentrations such as the distribution and availability of nutrients (e.g., Giesbrecht et al., 2018). Furthermore, more specific impacts of sea ice decline on water column phytoplankton (such as phytoplankton community composition and phytoplankton carbon biomass; Neeley et al., 2018) will be critical to continue to monitor.

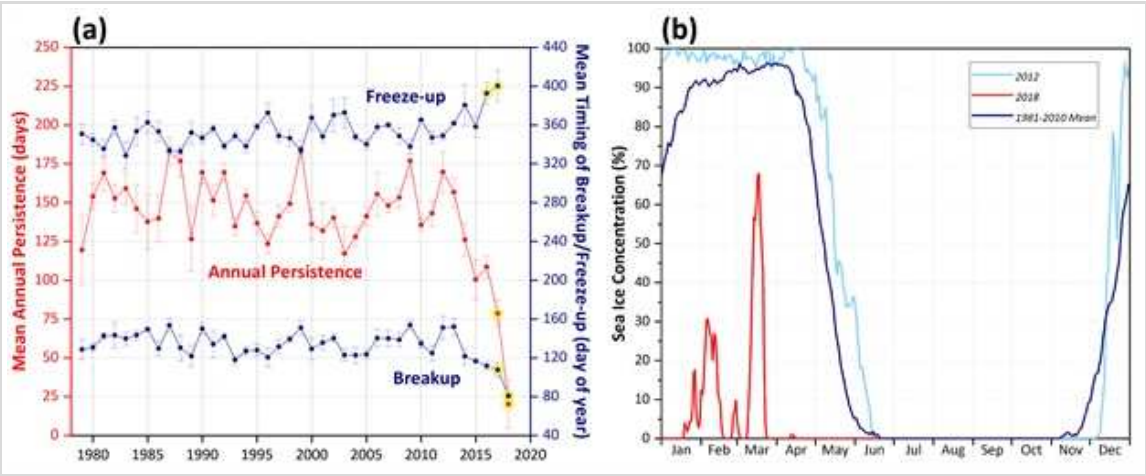

Fig. 4. (a) Sea ice variability (annual persistence and the timing of breakup/freeze-up) at the DBO1/SLIP region (see **Fig. 3** for location) from 1979 to 2018 (error bars as ±1 standard deviation depict spatial variability within the polygon) based on SMMR, SSM/I, and SSMIS data (Comiso et al., 2017a, b). See Frey et al. (2014, 2015) for further details of methodology. Circled in

yellow are the outliers identified using a double Grubb's test ($p < 0.0001$). (b) Daily time series of sea ice concentration at the DBO1/SLIP region, highlighting the 1981-2010 mean, 2012 (one of the highest years of sea ice cover on record), and 2018 (the lowest year of sea ice cover on record).

Primary Production

Chlorophyll-*a* concentrations give an estimate of the standing stock of algal biomass. Rates of primary production (i.e., the production of organic carbon via photosynthesis) provide a different perspective, and can be estimated by combining remotely sensed chlorophyll-*a* concentrations with sea surface temperatures, incident solar irradiance, and mixed layer depths. Estimates of ocean primary productivity for nine regions (and the average of these nine regions) across the Arctic, relative to 2003-17 base period, indicate above average primary productivity for 2018 in three regions and below average primary productivity in six regions as well as the overall Arctic region (**Fig. 5**, **Table 1**). Areas with the above average anomalies for 2018 include the Eurasian Arctic, the Bering Sea, and the Baffin Bay/Labrador Sea regions. In the longer term, positive trends in primary productivity occurred in all regions during the period 2003-18 (**Fig. 5**, **Table 1**). Statistically significant trends occurred in the Eurasian Arctic, Barents Sea, Greenland Sea, and North Atlantic, with the steepest trends found for the Barents Sea (12.85 g C/m^2/yr/dec, or a ~24.4% increase) and the Eurasian Arctic (12.74 g C/m^2/yr/dec, or a ~30.8% increase).

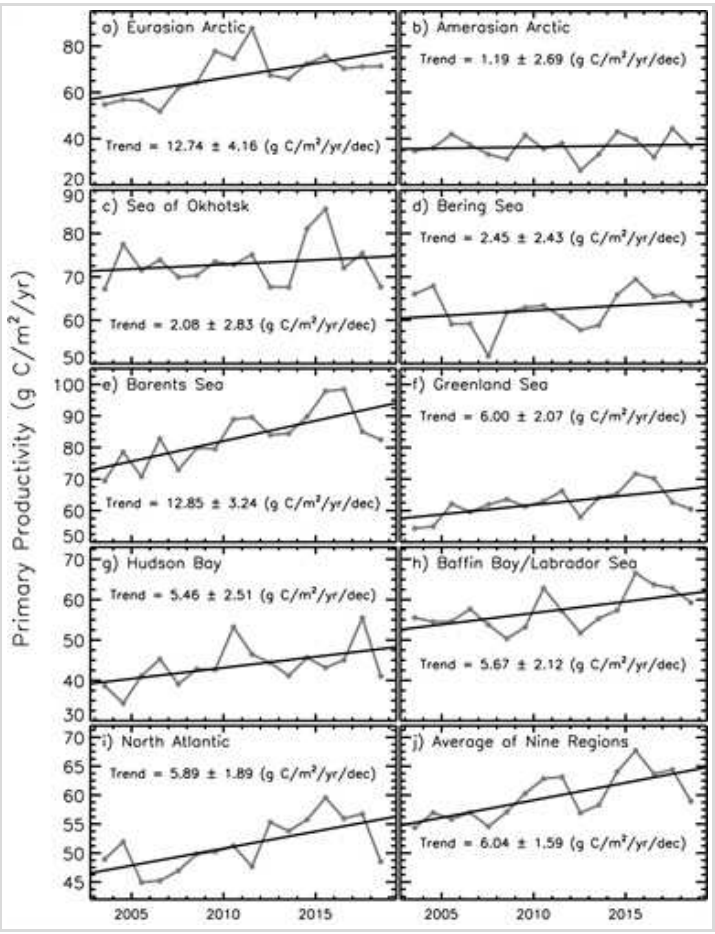

Fig. 5. Primary productivity (2003-18, March-September only) in nine different regions of the Northern Hemisphere (for a definition of the regions see Comiso (2015)), as well as the average of these nine regions, derived using chlorophyll-*a* concentrations from MODIS-Aqua data, the NOAA 1/4° daily Optimum Interpolation Sea Surface Temperature dataset (or daily OISST) that uses satellite sea surface temperatures from AVHRR, and additional parameters. Values are calculated based on the techniques described by Behrenfeld and Falkowski (1997) and represent net primary productivity (NPP). Additional information regarding these data can be found in **Table 1**.

Table 1. Linear trends, statistical significance, percent change, and primary productivity anomalies in 2018 (March-September) in the nine regions (and overall average) as shown in **Fig. 4**. Utilizing the Mann-Kendall test for trend, values in **bold** are significant at the 95% confidence level. The percent change was estimated from the linear regression of the 16-year time series.

Region	Trend, 2003-18 (g C/m^2/yr/decade)	Mann-Kendall *p*-value	% Change	2018 Anomaly (g C/m^2/yr) from a 2003-17 base period	2018 Primary Productivity (% of the 2003-17 average)
Eurasian Arctic	**12.74**	0.011	30.8	4.06	106.0
Amerasian Arctic	1.19	0.626	4.7	-0.10	99.7
Sea of Okhotsk	2.08	0.564	4.1	-5.75	92.2
Bering Sea	2.45	0.398	5.7	1.12	101.8
Barents Sea	**12.85**	0.001	24.4	-0.97	98.8
Greenland Sea	**6.00**	0.020	14.5	-2.11	96.6
Hudson Bay	5.46	0.064	19.3	-2.84	93.5
Baffin Bay/Labrador	5.67	0.064	15.0	2.13	103.7
North Atlantic	**5.89**	0.003	17.5	-3.08	94.0
Average of Nine	**6.04**	0.001	15.3	-0.84	98.6

While similar trends have been reported previously for these regions using both SeaWiFS and MODIS data (Comiso, 2015), satellite evidence does suggest that recent increases in cloudiness have dampened the increases in production that would have otherwise occurred as a function of sea ice decline alone (Bélanger et al., 2013). Further challenges remain with linking primary productivity, as well as depth-integrated chlorophyll biomass throughout the water column, to satellite-based surface chlorophyll-*a* values (Babin et al., 2015; Lee et al., 2015; Tremblay et al., 2015; Kahru, 2017). Satellite-based chlorophyll-*a* and primary productivity estimates continue to be confounded by issues such as river turbidity in coastal regions (e.g., Demidov et al., 2014; Chaves et al., 2015) and the presence of sea ice. Efforts to improve satellite retrieval algorithms based on in situ observations are thus critical to continue in all regions of the Arctic.

References

Ardyna, M., M. Babin, E. Devred, A. Forest, M. Gosselin, P. Raimbault, and J.-É. Tremblay, 2017: Shelf-basin gradients shape ecological phytoplankton niches and community composition in the coastal Arctic Ocean (Beaufort Sea). *Limnol. Oceanogr.*, 62, 2113-2132, doi: 10.1002/lno.10554.

Babin, M., S. Bélanger, I. Ellinsten, A. Forest, V. Le Fouest, T. Lacour, M. Ardyna, and D. Slagstad, 2015: Estimation of primary production in the Arctic Ocean using ocean colour remote sensing and coupled physical-biological models: Strengths, limitations and how they compare. *Prog. Oceanogr.*, 139, 197-220, doi: 10.1016/j.pocean.2015.08.008.

Barber, D. G., H. Hop, C. J. Mundy, B. Else, I. A. Dmitrenko, J. -É. Tremblay, J. K. Ehn, P. Assmy, M. Daase, L. M. Candlish, and S. Rysgaard, 2015: Selected physical, biological and biogeochemical implications of a rapidly changing Arctic Marginal Ice Zone. *Prog. Oceanogr.*, 139, 122-150, doi: 10.1016/j.pocean.2015.09.003.

Behrenfeld, M. J., and P. G. Falkowski, 1997: Photosynthetic rates derived from satellite-based chlorophyll concentration. *Limnol. Oceanogr.*, 42(1), 1-20.

Bélanger, S., M. Babin, and J. É. Tremblay, 2013: Increasing cloudiness in Arctic damps the increase in phytoplankton primary production due to sea ice receding. *Biogeosciences*, 10, 4087-4101, doi: 10.5194/bg-10-4087-2013.

Chaves, J., P. J. Werdell, C. W. Proctor, A. R. Neeley, S. A. Freeman, C. S. Thomas, and S. B. Hooker, 2015: Assessment of ocean color data records from MODIS-Aqua in the western Arctic Ocean. *Deep-Sea Res. Pt. II*, 118A, 32-43, doi: 10.1016/j.dsr2.2015.02.011.

Comiso, J. C., 2015: Variability and trends of the global sea ice covers and sea levels: Effects on physicochemical parameters, in *Climate*

*and Fresh Water Toxin*s. L. M. Botana, M. C. Lauzao, and N. Vilarino, Eds., De Gruyter, Berlin, Germany.

Comiso, J. C., R. Gersten, L. Stock, J. Turner, G. Perez, and K. Cho, 2017a: Positive trends in the Antarctic sea ice cover and associated changes in surface temperature. *J. Clim.*, 30, 2251-2267, doi: 10.1175/JCLI-D-16-0408.1.

Comiso, J. C., W. N. Meier, and R. Gersten, 2017b: Variability and trends in the Arctic Sea ice cover: Results from different techniques. *J. Geophys. Res. Oceans*, 122, 6883-6900, doi: 10.1002/2017JC012768.

Demidov, A. B., S. A. Mosharov, and P. N. Makkaveev, 2014: Patterns of the Kara Sea primary production in autumn: Biotic and abiotic forcing of subsurface layer. *J. Marine Syst.*, 132, 130-149, doi: 10.1016/j.jmarsys.2014.01.014.

Frey, K. E., J. A. Maslanik, J. Clement Kinney, and W. Maslowski, 2014: Recent variability in sea ice cover, age, and thickness in the Pacific Arctic Region, in *The Pacific Arctic Region: Ecosystem status and trends in a rapidly changing environment*. J. M. Grebmeier, and W. Maslowski, Eds., Springer: Dordrecht, pp. 31-64.

Frey, K. E., G. W. K. Moore, L. W. Cooper, and J. M. Grebmeier, 2015: Divergent patterns of recent sea ice cover across the Bering, Chukchi and Beaufort seas of the Pacific Arctic Region. *Prog. Oceanogr.*, 136, 32-49, doi: 10.1016/j.pocean.2015.05.009.

Giesbrecht, K. E., D. E. Varela, D. E., J. Wiktor, J. M. Grebmeier, B. Kelly, and J.E. Long, 2018 (in press): A decade of summertime measurements of phytoplankton biomass, productivity and assemblage composition in the Pacific Arctic Region from 2006 to 2016. *Deep Sea Res. Pt. II–Top. Stud. Oceanogr.*, doi: 10.1016/j.dsr2.2018.06.010.

Hill, V., M. Ardyna, S. H. Lee, and D. E. Varela, 2018: Decadal trends in phytoplankton production in the Pacific Arctic Region from 1950 to 2012. *Deep-Sea Res. Pt. II*, 152, 82-94, doi: 10.1016/j.dsr2.2016.12.015.

Kahru, M., 2017: Ocean productivity from space: Commentary. *Global Biogeochem. Cycles*, 31, 214-216, doi: 10.1002/2016GB005582.

Lee, Y. J., et al., 2015: An assessment of phytoplankton primary productivity in the Arctic Ocean from satellite ocean color/in situ chlorophyll-*a* based models. *J. Geophys. Res. Oceans*, 120, 6508-6541, doi: 10.1002/2015JC011018.

Leu, E., C. J. Mundy, P. Assmy, K. Campbell, T. M. Gabrielsen, M. Gosselin, T. Juul-Pedersen, and R. Gradinger, 2015: Arctic spring awakening - Steering principles behind the phenology of vernal ice algal blooms. *Prog.Oceanogr.*, 139, 151-170, doi: 10.1016/j.pocean.2015.07.012.

Moore, S. E., and J. M. Grebmeier, 2018: The Distributed Biological Observatory: Linking physics to biology in the Pacific Arctic region. *Arctic*, 71 (Suppl. 1), 1-7; doi: 10.14430/arctic4606.

Müller-Karger, F. E., R. Varela, R. Thunell, R. Luerssen, C. Hu, and J. J. Walsh, 2005: The importance of continental margins in the global carbon cycle. *Geophys. Res. Lett.*, 32, L01602, doi: 10.1029/2004GL021346.

Neeley, A. R., L. A. Harris, and K. E. Frey, 2018: Unraveling phytoplankton community dynamics in the northern Chukchi and western Beaufort seas amid climate change. *Geophys. Res. Lett.*, 45, 7663-7671, doi: 10.1029/2018GL077684.

Tremblay J. -É., L. G. Anderson, P. Matrai, S. Bélanger, C. Michel, P. Coupel, and M. Reigstad, 2015: Global and regional drivers of nutrient supply, primary production and CO_2 drawdown in the changing Arctic Ocean. *Prog. Oceanogr.*, 139, 171-196, doi: 10.1016/j.pocean.2015.08.009.

November 19, 2018